Structural Engineering and Mechanics, Vol. 3, No. 6 (1995) 593-609
DOI: http://dx.doi.org/10.12989/sem.1995.3.6.593

Finite element modelling of reinforced concrete structures with laboratory verification

Y.M. Cheng †

Department of Civil and structural Engineering, Hong Kong Polytechnic, Hong Kong

Abstract. The presence of reinforcement has a significant influence on the stress-strain behaviour of reinforced concrete structures, expecially when the failure stage of the structures is approached. In the present paper, the constrained and non-constrained zones of concrete due to the presence of reinforcement is developed and the stress-stress-strain behaviour of concrete is enhanced by a reinforcement confinement coefficient. Furthermore, a flexible method for the modelling of reinforcement with arbitrary orientation and not passing the nodes of concrete element is also proposed. Numerical examples and laboratory tests have shown that the coefficient and the modelling technique proposed by the author are satisfactory.

Key words: concrete; reinforcement; confinement; finite element.

1. Introduction

Since concrete is good in compression but weak in tension, reinforcement has to be used to take up the tensile stresses and inhibit the growth of cracks in concrete. For concrete structures subjected to corrosive environment, the development and propagation of cracks are very important and have to be considered carefully. For such a composite material with different nonlinear properties in compression and tension, analytical methods for describing the development and growth of cracks are not possible. Simplified methods are adopted for strength estimation while many empirical formulae are formulated for considering cracks in many building codes which is necessary for routine design. For critical structures like nuclear plant or major sewage treatment plant, finite element analysis is however considered to be necessary for a detailed study.

1.1. At present, reinforcement is usually modelled by the following models, One-dimensional steel bar element through concrete element nodes

This approach has been used by many early researchers, but its pronounced shortcoming is that the steel bar elements have to pass through nodes of concrete elements which are occasionally difficult to be achieved in structures with complicated reinforcement layout unless the layout of the mesh is also complicated.

1.2. The effective steel layered model

This approach is especially suitable to slab and shell structures where the reinforcement usually covers the whole concrete plan uniformly in layers. It is however difficult to be applied to problems

† Professor

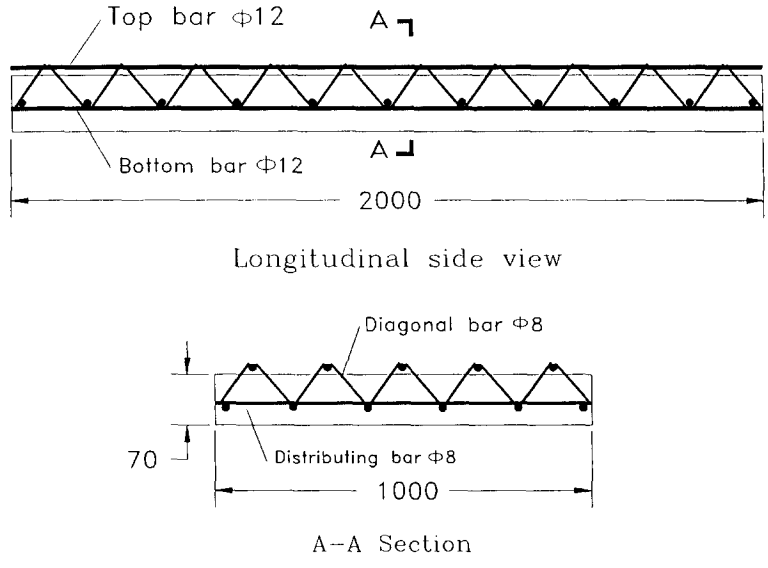

Fig. 1 Dimension of reinforced concrete truss plank.

with reinforcement oriented in arbitrary direction like the concrete truss plank as shown in Fig. 1.

1.3. Embedded representations for reinforcement

Phillips and zienkiewicz (1976) developed an embedded representation in which the virtual work integration is performed along the reinforcing laver and the reinforcement is aligned with one of the local isoparametric element coordinate axes but not passing through the nodes of concrete element. This description is better than the former 2 models but is still not suitable for reinforcement with arbitrary orientation.

1.4. Modified embedded representations for reinforcement

Elwi and Hrudey (1989) have presented a formulation for a general reinforcing bar embedded in general two-dimensional elements. The bar can be oriented with arbitrary direction and not passing the nodes of concrete element, i.e., independent of mesh. The author has extended the concept of Elwi to general three-dimensional elements with improvement and correction in the transformation process.

Due to the combined action of transverse and longitudinal reinforcement, deformation in concrete compressive zone may be confined by spatial frame action. This effect varies with the quantity and spacing of steel in the structure. Although two dimensional plane stress analysis is usually sufficient for the analysis of common reinforced concrete structures, a three dimensional stress state actually always exists. When this effect becomes significant enough, such as in columum with spiral reinforcement etc., it is necessary to consider it in test and strength calculation. The constraint action of reinforcement has also a significant effect on the development and propagation of cracks in concrete.

For the influence of reinforcement on the constitutive relation of concrete, yield and failure criterions etc., there are some common approaches which are:

(1) Increase of concrete ultimate strain.
(2) Application of Kent-Park σ-ε curve (Kupfer *et al.* 1969, 1970).
(3) Compound steel element, i.e., steel element is in axial-stress state as well as in bending state.
(4) Considering steel bar as a one-dimensional element, meanwhile, its confining effect on concrete is also put into account. This is the approach used by the authors in the present paper.

A brief discussion on these concepts can be summarized as follows. The ultimate strain ε_{cu} of concrete can be increased in the presence of reinforcement (especially stirrups) because of the restraint to the compressive strain of concrete at ultimate state which will improve the ductility of structures. ε_{cu} for reinforced concrete is hence greater than that of plain concrete. Unfortunately, this consideration can not be readily applied to quantitative analysis using the dimension and distribution of reinforcement. Several important parameters could be used to adjust the σ-ε curve for concrete with the presence of reinforcement which include ratio of stirrups volume and concrete volume surrounded by stirrups, spcing of stirrups, cover of concrete etc.. Such application in finite element analysis appeared to be not rewarding at present because more material parameters and complicated σ-ε relation are required. It is possible to describe reinforcement as a bending element as well as an axial-stress element. This approach is much more complicated to be used. In this paper, the author proposes an alternative in the formulation of the reinforcement stiffness matrix for one dimensional steel bar element with arbitrary direction and take into account the confining action of reinforcement by a confinement coefficient from the dimension and location of reinforcement.

2. Deformation of steel bar

Consider the reinforcement embedded in a concrete element as shown in Fig. 2. It is assumed that reinforcement element is in axial stress state and fine bonding exists between bars and surrounding concrete. Thus the local axial strain ε'_x along the bar is determined by the general

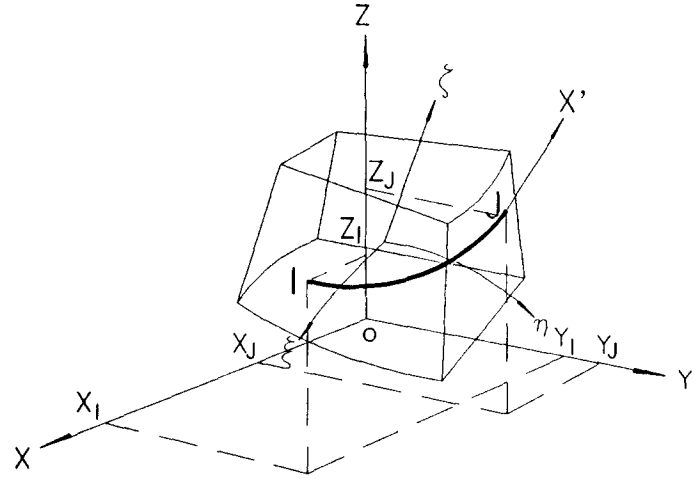

Fig. 2 Concrete element with steel bar.

concrete strain field as follows,

$$\varepsilon'_x = l^2\varepsilon_x + m^2\varepsilon_y + n^2\varepsilon_z + lm\gamma_{xy} + mn\gamma_{yz} + ln\gamma_{zy}$$

$$= (l^2 m^2 n^2 \;\; lm \;\; mn \;\; ln) \begin{bmatrix} \varepsilon_x \\ \varepsilon_y \\ \varepsilon_z \\ \gamma_{xy} \\ \gamma_{yz} \\ \gamma_{zx} \end{bmatrix} \tag{2.1}$$

where l, m, n are the directions of the steel bar. Eq. (2.1) can be exprssed in another form as

$$\begin{bmatrix} \varepsilon'_x \\ \varepsilon'_y \\ \varepsilon'_z \\ \gamma'_{xy} \\ \gamma'_{yz} \\ \gamma'_{zx} \end{bmatrix} = \begin{bmatrix} l^2 & m^2 & n^2 & lm & mn & ln \\ & & & 0 & & \end{bmatrix} \begin{bmatrix} \varepsilon_x \\ \varepsilon_y \\ \varepsilon_z \\ \gamma_{xy} \\ \gamma_{yz} \\ \gamma_{zx} \end{bmatrix}$$

i.e. $$\{\varepsilon'\} = [C]\{\varepsilon\} - [C][B]\{d\} = [B]\{d\} \tag{2.2}$$

where $[B]$ is the conventional strain displacement matrix
$[C]$ is the matrix in Eq.(2.2)
$\{d\}$ is the displacement vector
$[\underline{B}] = [C][B]$ = strain displacement matrix for the steel bar

The stress-strain relation for the reinforcement bar is given by

$$\begin{bmatrix} \sigma'_x \\ \sigma'_y \\ \sigma'_z \\ \tau'_{xy} \\ \tau'_{zx} \\ \tau'_{zx} \end{bmatrix} = \begin{bmatrix} E & 0 & 0 & 0 & 0 & 0 \\ & & & 0 & & \end{bmatrix} \begin{bmatrix} \varepsilon'_x \\ \varepsilon'_y \\ \varepsilon'_z \\ \gamma'_{xy} \\ \gamma'_{yz} \\ \gamma'_{zx} \end{bmatrix}$$

i.e. $$\{\sigma'\} = [D']\{\varepsilon'\} \tag{2.3}$$

In the six stress components as shown in Eq. (2.3), only the term σ'_x is not equal to zero. From Eqs. (2.2) and (2.3), it follows that:

$$\{\sigma'\} = [D'][C]\{\varepsilon\} = [D'][C][B]\{d\} \tag{2.4}$$

The stress $\{\sigma'\}$ and strain $\{\varepsilon'\}$ in the local axes can be determined from Eqs. (2.1) to (2.4) and can be transformed to global axes easily. The stress in the steel bar is expressed in a special way in Eqs. (2.3) and (2.4) because we want the formulation of the stiffness matrix for the steel bar to resemble that of the concrete element and that the reinforcement can be located in any position in the concrete element.

The stiffness matrix of a concrete element containing reinforcement is given by:

$$K^{(e)} = \int_{\Omega_{concrete}} [B^{(e)}]^T [D][B^{(e)}] d\Omega + \int_{\Omega_{reinforcement}} [B^{(e)}]^T [\underline{D}][B^{(e)}] d\Omega$$

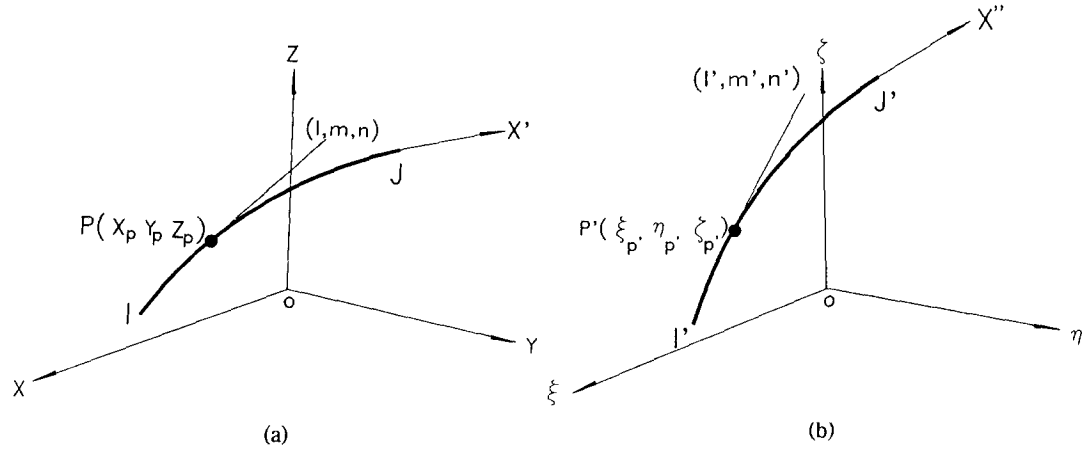

Fig. 3a Steel bar in global coordinate. b Steel bar in local coordinate.

$$= K_c^{(e)} + K_r^{(e)} \tag{2.5}$$

The first term in Eq. (2.5) is the contribution of concrete to the element stiffness matrix which is given by the conventional way. The second term in Eq. (2.5) represents the contribution of the steel bars to the element stiffness matrix. It can be expressed by Eq. (2.6) as

$$K_r^{(e)} = \sum_{i=1}^{Nr} A_i \int_{X_I}^{X_J} [B^{(e)}]^T [\underline{D}][B^{(e)}] dx' \tag{2.6}$$

where Nr is number of steel bars in element e
A_i is area of steel bar i
x' is curved coordinate as shown in Fig. 3a
X_I, X_J are the coordinates of the two ending points referring to the global axes
$[B]$ = conventional strain displacement matrix for isoparametric element

$$[\underline{D}] = [C]^T [D'][C]$$

$$[\underline{D}] = E \begin{bmatrix} l^4 & l^2m^2 & l^2n^2 & l^3m & mnl^2 & nl^3 \\ & m^4 & m^2n^2 & lm^3 & m^3n & m^2ln \\ & & n^4 & lmn^2 & n^3m & n^3l \\ & & & l^2n^2 & lm^2n & l^2mn \\ \textit{symmetry} & & & & m^2n^2 & mn^2l \\ & & & & & l^2n^2 \end{bmatrix} \tag{2.7}$$

It is noted that a full matrix $[\underline{D}]$ is obtained for the global constitutive matrix as compared with that in the local axes $[D]$. The direction cosines of any point P on the steel bar can be obtained easily by the orientation of the reinforcement.

The term dx' in Eq. (2.6) can be replaced by the following formula from Fig. 3a as

$$dx' = \frac{dx}{l} = \frac{dy}{m} = \frac{dz}{n} \tag{2.8}$$

In the local coordinate system as shown in Fig. 3b, dx'' is given by

$$dx''=\frac{d\xi}{l'}=\frac{d\eta}{m'}=\frac{dz}{n'} \tag{2.9}$$

where l', m', n' are direction cosines of point P in local coordinate which will be discussed in details later. Using Eqs. (2.8) and (2.9), an important relationship relating the local and global coordinates is obtained as,

$$\begin{aligned} dx'=\frac{dx}{1}&=\left(\frac{\partial x}{\partial\xi}=d\xi+\frac{\partial x}{\partial\eta}d\eta+\frac{\partial x}{\partial\xi}d\xi\right)/1 \\ =\frac{dx''}{1}&=\left(\frac{\partial x}{\partial\xi}=l'+\frac{\partial x}{\partial\eta}m'+\frac{\partial x}{\partial\xi}n'\right) \end{aligned} \tag{2.10}$$

With Eq. (2.10), Eq (2.6) can be rewritten as follows,

$$\begin{aligned} K_r^{(e)}&=\int_{\Omega_{reinforcement}}[B^{(e)}]^T[\underline{D}][B^{(e)}]d\Omega \\ &=\sum_i^{Nr}A_i\int_{j_1}^{\xi_J}[B^{(e)}]^T[\underline{D}][B^{(e)}]\times\frac{dx''}{l}\left(\frac{\partial x}{\partial\xi}l'+\frac{\partial x}{\partial\eta}m'+\frac{\partial x}{\partial\xi}n'\right) \end{aligned} \tag{2.11}$$

As seen in Eq. (2.11), this integration can be obtained if any point referring to the global coordinate system. Yamaguchi (1991) presented an approach using a lower-order element by simple mathematical manipulation and Elwi and Hrudey (1989) presented an approach associated with higher-order element by an iterative procedure. The mixed iteration process which wil be discssed in the following section can be viewed as an extension of the works by Elwi. From co-ordinate transformation, we have

$$\begin{bmatrix} dx \\ dy \\ dz \end{bmatrix}=\begin{bmatrix} \frac{\partial x}{\partial\xi} & \frac{\partial x}{\partial\eta} & \frac{\partial x}{\partial\xi} \\ \frac{\partial y}{\partial\xi} & \frac{\partial y}{\partial\eta} & \frac{\partial y}{\partial\xi} \\ \frac{\partial z}{\partial\xi} & \frac{\partial z}{\partial\eta} & \frac{\partial z}{\partial\xi} \end{bmatrix}\begin{bmatrix} d\xi \\ d\eta \\ d\xi \end{bmatrix}$$

$$i.e.,\ \{dX\}=[J]\{d\Omega\} \tag{2.12}$$

Inverting Eq (2.12), we have

$$\{d\Omega\}=[J]^{-1}\{dX\} \tag{2.13}$$

Eq. (2.13) can be rewritten in an incremental form as

$$\{\Delta\omega\}=[J]^{-1}\{\Delta X\} \tag{2.14}$$

Now the essential steps in the solution process can be summarized as follows.

Stage 1 Suppose one point P with its coordinate value (X_p, Y_p, Z_p) is given. The following quantities are evaluated:

(a)
$$\begin{aligned} X_0&=\Sigma N_i(0,\ 0,\ 0)X_i \\ Y_0&=\Sigma N_i(0,\ 0,\ 0)Y_i \\ Z_0&=\Sigma N_i(0,\ 0,\ 0)Z_i \end{aligned}$$

which is the values of the coordinates of the origin of the local coordinate system ξ-η-ξ in the global coordinate system.

(b) The trial direction cosines given below are evaluated as.

$$L=\left((X_p-X_0)^2+Y_p-Y_0)^2+(Z_p-Z_0)^2\right)^{1/2}$$
$$l_0=\frac{X_p-X_0}{L}$$
$$m_0=\frac{Y_p-Y_0}{L}$$
$$n_0=\frac{Z_p-Z_0}{L}$$

(c) If $L\to 0$, then $\xi_p=0$, $\eta_p=0$ and $\xi_p=0$ and stop here (converged), otherwise continue the following steps.

(d) Divide L into N sections, saly $N=100$, and $\Delta L=$ L/n,

$$\Delta X=\Delta L\cdot l_0$$
$$\Delta Y=\Delta L\cdot m_0$$
$$\Delta Z=\Delta L\cdot n_0$$

(e) set iteration counter $k=0$

set $\xi_k=\eta_k=\xi_k=0$,

set $X_k=X_0$, $Y_k=Y_0$, $Y_k=Y_o$, $Z_k=Z_0$.

Stage 2 $L=\left((X_p-X_k)^2+(Y_p-Y_k)^2+(Z_p-Z_k)^2\right)^{1/2}$

IF $L\to 0$, then $p=k$, $p=k$ and $p=k$ and stop here (converged), otherwise continue.

Stage 3. From (2.14)

$$\begin{bmatrix}\Delta\xi_k\\ \Delta\eta_k\\ \Delta\xi_k\end{bmatrix}=[J]_k^{-1}\begin{bmatrix}\Delta X\\ \Delta Y\\ \Delta\zeta\end{bmatrix} \tag{2.15}$$

Stage 4. Compute the followings terms and the corrector

$$X_k'=\Sigma N_j^k X_j$$
$$Y_k'=\Sigma N_j^k Y_j$$
$$Z_k'=\Sigma N_j^k Z_j \tag{2.16}$$

Because of the error produced from linear approximation, (X_k, Y_k, Z_k) is not exactly equal to (X_k', Y_k', Z_k') and a modification as given by Eq. (2.17) is required.

$$\begin{bmatrix}\Delta X'\\ \Delta Y'\\ \Delta Z'\end{bmatrix}=\begin{bmatrix}X_k-X_k'\\ Y_k-Y_k'\\ Z_k-Z_k'\end{bmatrix} \tag{2.17a}$$

and

$$\begin{bmatrix}\Delta\xi_k'\\ \Delta\eta_k'\\ \Delta\xi_k'\end{bmatrix}=[J]_k^{-1}\begin{bmatrix}\Delta X'\\ \Delta Y'\\ \Delta Z'\end{bmatrix} \tag{2.17b}$$

Therefore

$$\begin{bmatrix} \xi_{k+1} \\ \eta_{k+1} \\ \zeta_{k+1} \end{bmatrix} = \begin{bmatrix} \xi_k \\ \eta_k \\ \zeta_k \end{bmatrix} + \begin{bmatrix} \Delta\xi_k \\ \Delta\eta_k \\ \Delta\zeta_k \end{bmatrix} + \begin{bmatrix} \Delta\xi_k' \\ \Delta\eta_k' \\ \Delta\zeta_k' \end{bmatrix} \tag{2.17c}$$

and

$$\begin{bmatrix} X_{k+1} \\ Y_{k+1} \\ Z_{k+1} \end{bmatrix} = \begin{bmatrix} X_k \\ Y_k \\ Z_k \end{bmatrix} + \begin{bmatrix} \Delta X \\ \Delta Y \\ \Delta Z \end{bmatrix} \tag{2.17d}$$

go to Stage 2 and continued the iteration.

The direction cosines of steel bar in global coordinate, *i.e.*, (l, m, n), can be defined by the following if its curve axis is given,

$$\begin{bmatrix} l \\ m \\ n \end{bmatrix} = \begin{bmatrix} \frac{\partial x'}{\partial x}/L \\ \frac{\partial x'}{\partial y}/L \\ \frac{\partial x'}{\partial z}/L \end{bmatrix} \quad \mathrm{L} = \left[\left(\frac{\partial x'}{\partial x}\right)^2 + \left(\frac{\partial x'}{\partial y}\right)^2 \left(\frac{\partial x'}{\partial z}\right)^2\right] \tag{2.18}$$

Curved steel bar is usally described by straight line, parabola or arc which can be expressed using three points, namely, starting point, ending point and any other point near middle part of steel bar. Similary, the coordinate of curved steel bar in local coordinate can also be expressed by a parabola of its three critical point ξ_i, ξ_j and another point corresponding to that in global coordinate as follows,

$$\begin{bmatrix} l' \\ m' \\ n' \end{bmatrix} = \begin{bmatrix} \frac{\partial x''}{\partial \xi}/L' \\ \frac{\partial x'}{\partial \eta}/L' \\ \frac{\partial x'}{\partial \zeta}/L' \end{bmatrix} \quad \mathrm{L} = \left[\left(\frac{\partial x''}{\partial \xi}\right)^2 + \left(\frac{\partial x''}{\partial \eta}\right)^2 \left(\frac{\partial x''}{\partial \zeta}\right)^2\right]^{1/2} \tag{2.19}$$

For sake of convenience, the steel bar can be divided into several segments and linear approximation and interpolation can be employed to determine the direction cosines of the steel bar in the local coordinate system. In computer programming, a pre-processor can be employed to deal with this part of calculation before the main program starts, and this approcah has been adopted by the author. The advantage of the present approach as compared with that by Elwi is the correction of the present approach as compared with that by Elwi is the correction of the deviation from linear approximation which can be critical for curved bars. Even if curved steel bar is not present, this method is still appealing because the steel bar can be oriented in arbitrary direction but not passing the nodes of the three-dimensional concrete element while the method by Elwi is limited to two-dimensional problems only.

3. Analysis of influence from reinforcement constraint

There are many laboratory tests and theoretical studies on effective constrained zone of reinforcement in tensile zone of concrete. Such constraint is empirically incorporated into formulae

for spacing of cracks or bond slip for the control of crack width. This confinement can be produced by the transverse reinforcement (secondary bars or stirrups) and by contribution of residual tensile strength of crack concrete (tension stiffening). Giuriani *et al. (1991)* based on some rigorous assumptions and test analysis proposed a series of empirical equations concerned with two confining action due to the trnsverse reinforcement and the residual tensile stress transmitted by the faces of crack. In finite element analysis, however, crack phenomenon is generally modeled by smeared model which neglects the influence of crack width on the geometry of structures. In this paper, the confining action of reinforcement on concrete compressive zone is considered by the use of a confinement coefficient. Some basic and reasonable assumptions about the confining action can be set out as follows,

(1) The nearer the reference point (gauss point) of concrete and steel bars, the stronger will be the confining action.
(2) The larger the diameter of steel bars, the stronger will be the confining action.
(3) The more uniform distribution of the reference points of reinforcement around concrete, the stronger will be the confining action.
(4) The denser the reinforcement, the stronger will be the confining action.
(5) The more reinforcement presence in an element, the stronger will be the confining action.

A confinement coefficient which can reflect the above assumption can be readily written below as,

$$\phi_{cj}=\alpha\left(\frac{1}{\mu_{cj}}\right)^{\beta} \tag{3.1}$$

$$\mu_{cj}=\gamma N_{sj}\left[\sum_{i}^{N_{sj}}\left(\frac{D_i}{L_{ij}}\right)\right]\times\frac{1}{c_{vj}} \tag{3.2}$$

where ϕ_{cj} — influence coefficient

μ_{cj} — confining coefficient of reinforcement in reference point j of concrete in one element. When no reinforcement is in the element, set μ_{cj} to 1.0.

D_i — diameter of bar in reference point i in the same element which combined with L_{ij} based on assumption 2 and 3

L_{ij} — distance between reference point i of reinforcement and reference point j of concrete in the same element

C_{vj} — deviation coefficient of reinforcement distribution which reflecting assumption 4 can be determined by formula (3.3). When no reinforcement is in the element, set C_v to 1.0.

$$C_{vj}=\frac{\sigma}{\hat{L}} \tag{3.3}$$

$$\sigma=\sqrt{\frac{\Sigma(L_{ij}-\hat{L})^2}{N_{sj}}} \tag{3.4}$$

$$\hat{L}=\frac{\Sigma L_{ij}}{N_{sj}} \tag{3.5}$$

N_{sj} — total number of reference points of steel bars in one element based on assumption 5

α, β, γ — parameters, generally, $\gamma=1.0$, $\alpha=0.4$-0.5, $\beta=1/3$-$1/5$, which can be obtained by trial and error from several computations so that $\phi_{cj}=1.0$ without reinforcement and $\phi_{cj}=0.4$

with significant reinforcement

In the present work, cracked concrete is modeled by the smeared crack model. Concrete in tension is modeled as a linear elastic strain-softening material and the maximum tensile stress criterion will be employed to distinguish elastic behaviour from tensile fracture. The present work is an extension of that by Hinton (1988) and the elasto-viscoplastic model for concrete and steel followed that adopted by Hinton with the modification given in the follow sections.

The yield surface F_0 defines the onset of viscoplastic behavior and the strength limit surface F_f defines the intiation of material degradation. In Hintons, (1988) study, these functions are described in terms of the first and second deviatoric stress invariants I_1 and J_2 only which can be expressed as

$$F_0(\sigma,\ \sigma_0)=CI_1+(c^2I_1^2+3\beta J_2)^{1/2}-\sigma_0=0$$
$$F_f(\sigma,\ \sigma_f)=CI_1+(c^2I_1^2+3\beta J_2)^{1/2}-\sigma_f=0 \tag{3.6}$$

Typical values of c equal to 0.1775 and β equal to 1.355 have been adopted by Kupfer, Hilsdorfand Rush (1969). Inelastic volume dilation is kown to occur in concrete material near the ultimate stress. This kind of dilation, however, may be confined by transverse and longitudinal reinforcement, especially in cyclic loading or dynamic response. Therefore, a modification to invariant I_1 can be written as,

$$\bar{I}_1=\phi_{cj}(\sigma_1+\sigma_2+\sigma_3) \tag{3.7}$$

Eq. (3.6) keeps in original forms with $\bar{I}_1$ replaced by I_1 in Eq. (3.7). During inelastic straining, both surfaces F_0 and F_f change which depend on the amount of the accumulated damage expressed as the viscoplastic energy density W_p.

$$F_0(\sigma,\ \sigma_0(W_p,\ k))=0$$
$$F_f=(\sigma,\ \sigma_f(W_p))=0 \tag{3.8}$$

where $\sigma_0(W_p,\ K)$ defines the change of the yield stress level in uniaxial compression σ_0,
$\sigma_f(W_p)$ defines the change of the failure stress level in uniaxial compression σ_f,
W_p is the viscoplastic energy density defined as

$$W_p=\int_0^t \sigma^T \phi_{cj}\dot{\varepsilon}_{vp}dt \tag{3.9}$$

k is the viscoplastic work density in the softening range. It is defined as

$$k=W_p-W_p^f=\int_{t_f}^t \sigma^T \phi_{cj}\dot{\varepsilon}_{vp}dt \tag{3.10}$$

and t_f and W_p^f are the time and viscoplastic energy density when the strength limit is reached. In the present study, the constitutive behaviour of concreate under compression is given by

$$\begin{array}{ll} \sigma\le 0.5f_{cu} & \text{elastic} \\ 0.5\ f_{cu}<\sigma\le 0.75\ f_{cu} & H'=0.33 \\ 0.75\ f_{cu}<\sigma\le f_{cu} & H'=0.11 \\ \sigma=f_{cu} & H'=0 \end{array} \tag{3.11}$$

where H' is the hardening parameter

An exponential function will be used to describe the post-failure behavior. The function $\sigma_0(W_p,\ k)$ is defined by the expression,

Table 1 Material parameters (units in *N, mm*).

Material Property	Concrete	Steel
E	28.4E3	200E3
ν	0.2	/
f_c' or f_y	34.0	280.0
ε_u	0.0035	/
f_t	3.4	280.0
G_f	0.1	/
α	0.4	in eqs. (3.1),
β	1/5	and (3.2)
γ	1.0	

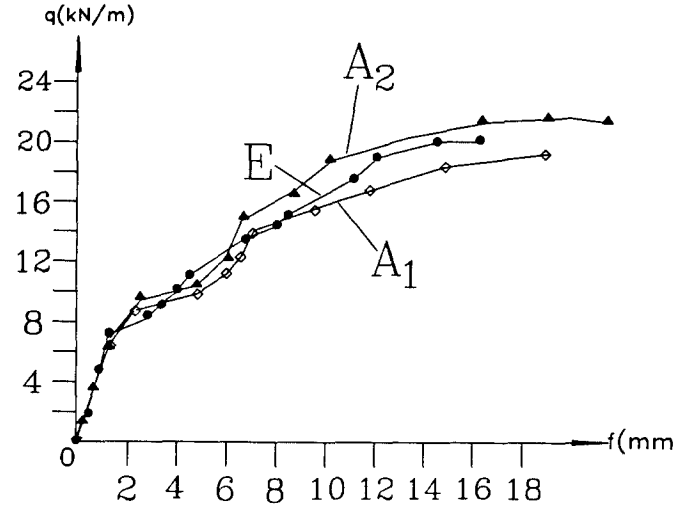

Fig. 4 Loading-maximum displacement.

$$\left.\begin{aligned} &\sigma_0(W_p,\ k)=\alpha_1 f'_c \\ &\sigma_0(W_p,\ k)=\alpha_1 f_c'+H_1'\bar{\varepsilon} \\ &\sigma_0(W_p,\ k)=\alpha_2 f_c'+H_2'\bar{\varepsilon} \\ &\sigma_0(W_p,\ k)=f_c' \end{aligned}\right\} \quad W_p \le W_p^f$$

$$\text{where}\quad \bar{\varepsilon}=\psi\sqrt{\Sigma(\varepsilon_{ij})^2}$$

$$\left.\begin{aligned} &\sigma_0(W_p,\ k)=\alpha_1 f_c'\exp(-\alpha_c k) \end{aligned}\right\} \quad W_p > W_p^f \qquad (3.12)$$

in which α_1 defines the limit for elastic behavior (typically $\alpha_1=0.4-0.5$), α_2 defines linear hardening position ($\alpha_2=0.7-0.8$) and α_c models the degradation after failure ($\alpha_c=10-50$). H_1' and H_2' are plastic modulus ($H_1'\approx 1/3E$, $H_2'\approx 1/9E$). The parameter f_c' is the static compressive strength of concrete. Ψ is equal to 2/3 under loading and $-2/3$ under unloading.

The failure stress will be assumed to be a linear function of the viscoplastic energy density, and the function $\sigma_f(W_p)$ is defined by the expression

$$\sigma_f(W_p)=\beta_0 f_c'(1-\beta_1-W_p) \qquad 0<W_p\le W_p^f \qquad (3.13)$$

The parameter β_0 and β_1 are determined from experiments. From [1], β_0 is from 1.836 to 2.291 and β_1 is from 0.792 to 2.365.

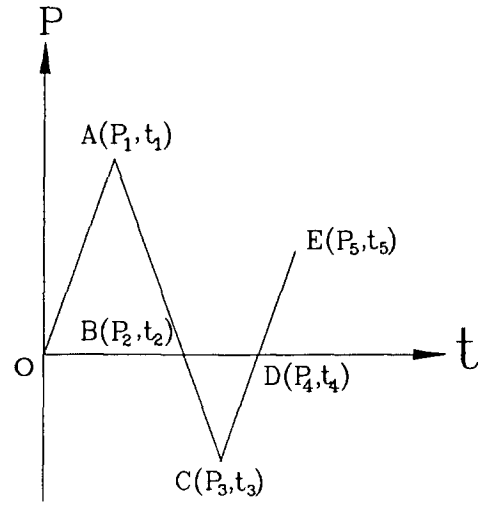

Fig. 5 Loading history.

The computer program used by the author is based on that by Hinton (1988) with major improvement in the reinforcement modelling technique and considered the concrete confinement coefficient as mentioned before. The use of Fortran 90 with dynamic data management is also adopted in the enhancement of this program.

4. Numerical study of reinforcement truss plank

4.1 Static Example

The problem under consideration is the 1×2 m composite reinforcement truss concrete plank as shown in concrete. During the load tests, the two edges of the plank was simply supported and a uniform line load was applied at the center. Due to symmetry, only one-quarter of structure needs to be considered in analysis. Some parameters for the tests are shown as following Table 1.

From Fig. 4, we see that two analytical results with and without confining action represented by $A1$ and $A2$ respectively fit experimental result represented by E very well before yield of structure. The two analytical curves almost overlap due to the model assumption that before concrete yields, confining action plays no role in structural behavior. Obvious difference amongst the three results appears after many concrete gaussian points have yielded. $A2$ fits better E than $A1$, which means that confining action of reinforcement is important and should be considered in analysis. The confinement coefficient proposed by the author appears to be reasonable from this study.

4.2. Dynamic example

In situation where it is difficult if not impossible to simulate the effect of dynamic loads acting on a structure by using equivalent static loads, analysis methods have to be employed which take into account the important dynamic effects. These methods are based on classical

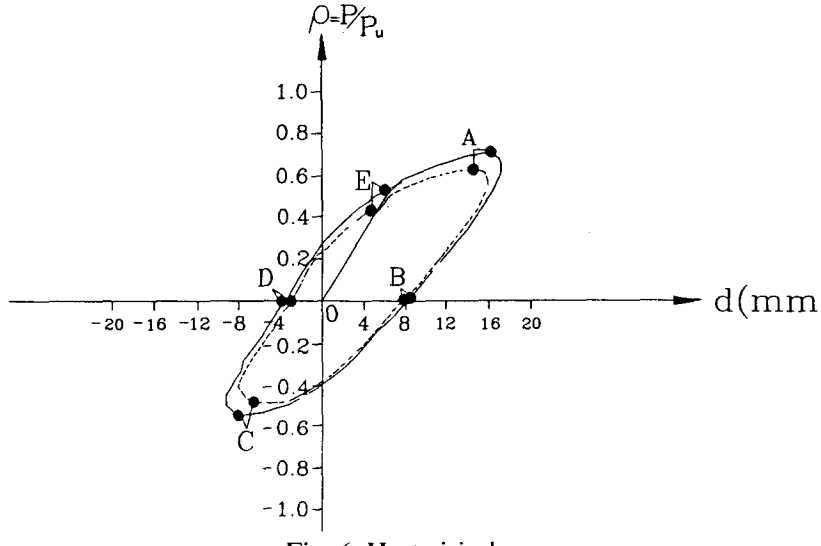

Fig. 6 Hysterisis loop.

theory of vibrations and structural dynamics. For lumped parameter system such as those resulting from a finite element discretization, the equations of motion can be written in matrix forms as

$$[M]\{\ddot{x}\}+[C]\{\dot{x}\}+[K(x,t)]\{x\}=\{P(t)\} \tag{4.1}$$

Here in this paper predictor-corrector form of Newmark's method has been recommended (Hinton 1988). The sample is described as above, but the loading system is specially designed as shown in Fig. 5.

In finite elemtnt programming, stress state of a specific reference point in every element is either in elastic state, one-way crack, two-way crack, yield, failure, crushed etc. determined by a series of criterions. The load history adopted in the present study is sown in Fig. 5. Point A (P_1, t_1) is obtained at the time when the total number of yielded gauss points in proportional to total number gauss points up to a specific limit, *i.e.*,

$$\frac{N_{gy}}{N_g \times N_{ele}} \geq \rho_{limit}$$

where N_{gy} is number of yielded gauss points of concrete
N_g is number of gauss point of concrete, in reduced integration scheme, $N_g=15$ for 20 nodes brick element
N_{ele} is nuber of element
ρ_{limit} is a specific limit, $\rho_{limit}=0.02$-0.06

When A (P_1, t_1) is given, extends t_1 to t_2 such that $t_2=2t_1$ and $P_2=0$, thus we obtain point B (P_2, t_2). Stretching AB to C and set P_3 to $-0.6P_1$. After simple deduction, t_3 can be obtained as $2.6t_1$. Repeating the above procedure, point D (P_4, t_4) in loading history is readily determined with $P_4=0$ with $t_4=3.2t_1$, and $E(P_5, t_5)$ with $P_5=0.6P_1$ and $t_5=3.8t_1$.

Because loading period is much longer than the fundamental period of the plank, therefore, the above loading system is similar to cyclic loading. Fig. 6 shows a relationship of loading

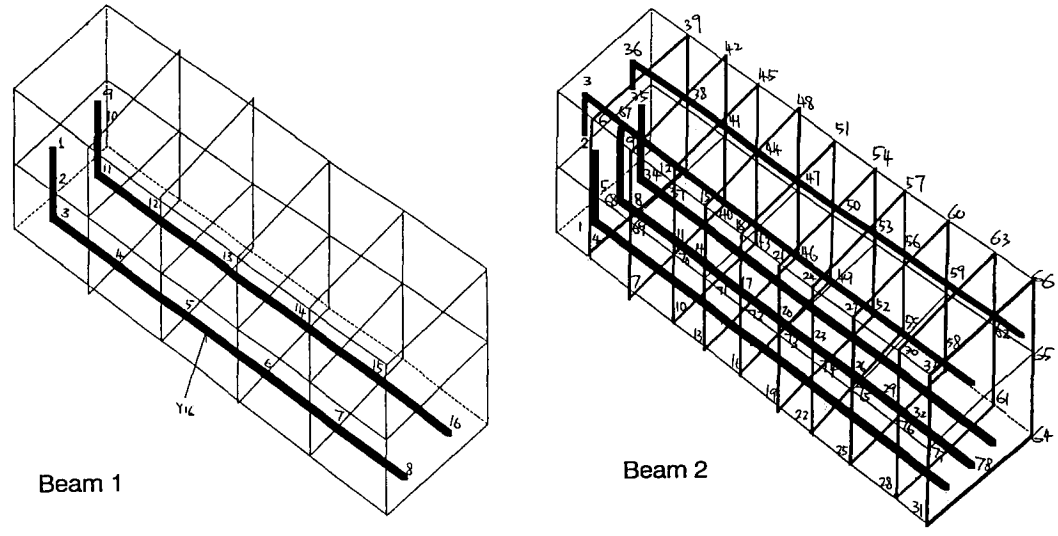

Fig. 7 Finite Element Model for Two Beams.

Table 2 Material Properties (units in *N, mm*)

Material Property	Concrete	Steel bar
E	28.4E3	200E3
ν	0.2	/
f_{cu} or f_y	50.0	280.0
ε_u	0.0035	/
f_t	3.4	280.0
G_f	0.1	/

and displacement hysteresis curve in which the two curves are translated form of loading-time history and displacement-time result. The loading system is designed in this way so that influence of confining action on hysteresis loop, which reflects energy absorption, can be shown because more loading has to be added to the structures under consideration of reinforcement on plastic behavior of concrete (the same quantities of gauss point yield are reached in these two cases).

A final conclusion is that maximum displacement dosen't occur at the moment of maximum load acted on plank because inertia forces play a part in dynamic analysis. It is near to the maximu loading due to the fact that loading period is much longer than structural fundamental period which is around 4 second and the loading is similar to static loading. Pronounced difference occurred shortly after many gaussian points of concrete have yielded which is similar to that in the static example above. For this specially designed loading system, unloading point A in loading history of thw two situmation A_1 and A_2 is not the same which can be explained by the confining action of reinforcement which increases the yield level so that A_1 has a higher P_1 in loading history than A_1 for the same unloading criterion ρ_{limit}.

5. Laboratory and numerical study on reinforced concrete beam

Two simply supported concrete beams of 3 m span length are loaded with a point load at

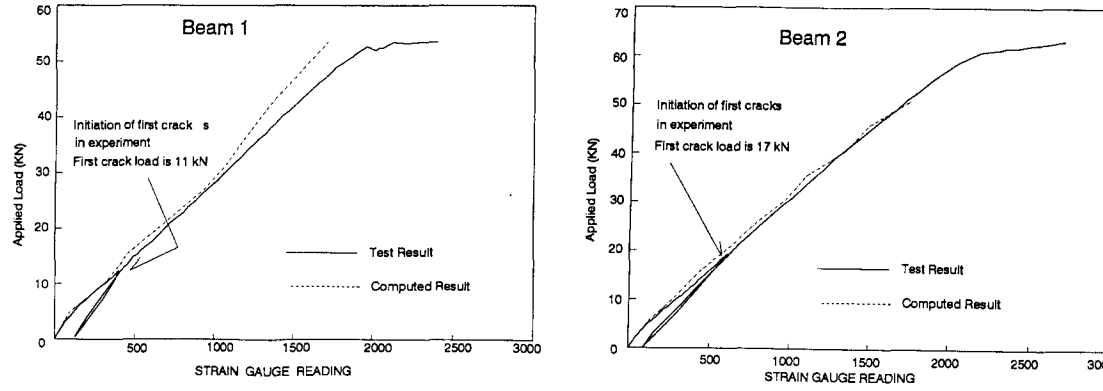

Fig. 8 Relation between Strain and Load.

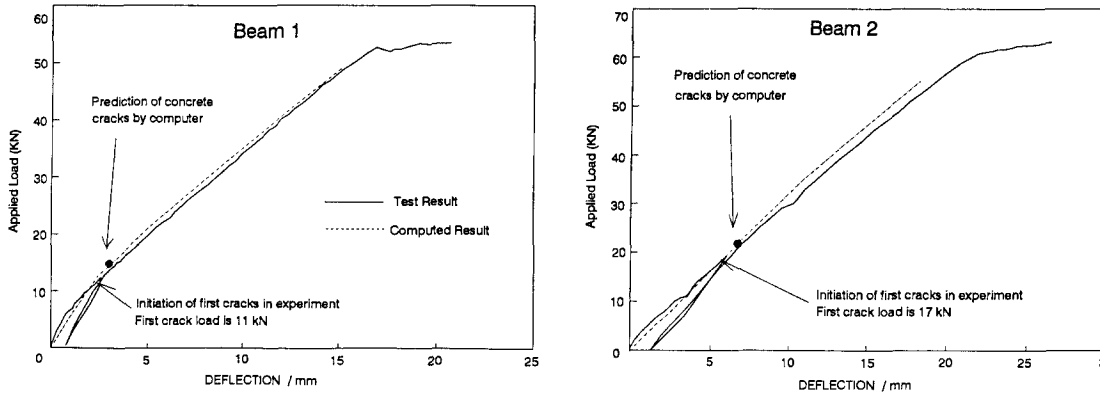

Fig. 9 Relation between Deflection and Load.

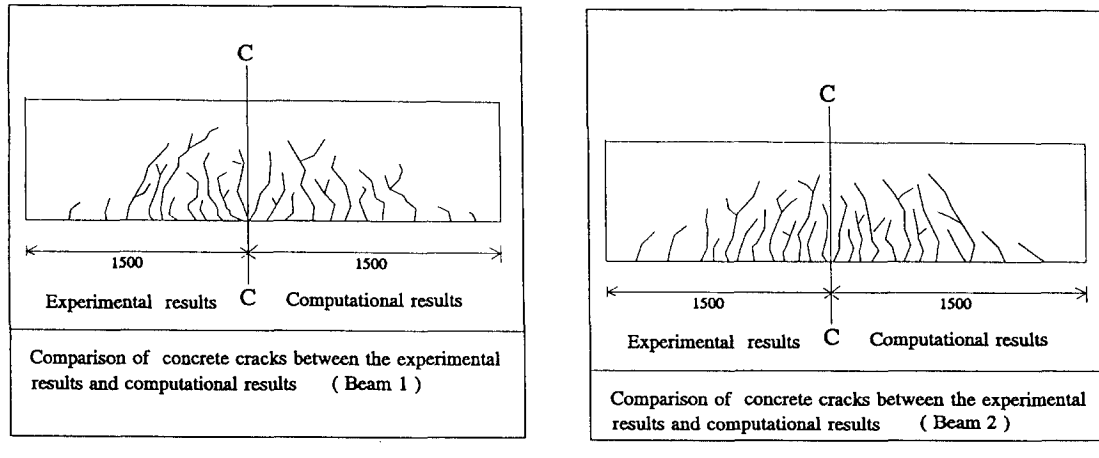

Fig. 10 Crack Pattern of the two Beams.

the middle of the beams. Relation of the applied load with deflection and stresses in reinforcement and concrete as well as the development and propagation of cracks are monitored during the tests. The dimension of the beams are 150 mm wide and 220 mm deep. The first beam is reinforced with 2 number of 16 mm diameter high yield bars without ny stirrup. The second beam is reinforced with three number of 16 mm diameter high yield bars at the bottom, 2 number of 8 mm mild steel bars at top and 6 mm diameter mild steel stirrup at 100 nm spacing. The cover to the reinforcement are 25 mm to the two beams. In the design of the reinforcement for the two beams, they are designed to carry the same ultimate load using the code BS 8110. The second beam requires more reinforcement because its has smaller lever arm as compared with the first beam.

The beams are modelled with 10 number of 20 nodes brick elements and 108 nodes. Due to symmetry, only half of the section is considered in analysis. The beam is divided into half along its mid-depth so that there are totally 2 layers of brick elements and each layer composed of 5 regular brick elements. 15 Gaussian points are on the surface of the elements. It is interesting to note that the same finite elemnt mesh can be adopted for the two beams even though these two beams possessed different number of steel bars with different layout. This is possible because of the numerical modelling techniques as discussed proviously. The finite element model used for the present analysis is shown in Fig. 7. The material parameters used for the present analysis is shown in Table 2.

The relation between the maximum compressive strain at top fiber and the applied load at the mid-section of the beam is shown in Fig. 8. It is encouraging to note that the prediction of strain with the measured result is rather good for the two beams. Furthermore, beam 2 has a higher first crack load as well as greater ultimate load as compared with beam 1. This is mainly due to the presence of stirrups in beam 2 which has helped to confine the concrete and hence a three-dimensional stress state is achieved. Since concrete has a greater strength under a three-dimensional stress state, beam 2 should show greater strength as compared with beam 1 and this is obtained in the present study. The top compression reinforcements in beam 2 have only minor contribution because they are small and are mild steel bars. In the present study, the effect of the top bar is smaller than that of stirrup but this may not be the case for other problems.

The relation between the maximum deflection and the applied load is shown in Fig. 9. It is noticed that the prediction of the initial crack load is very similar to that obtained from the test. Looking at Figs. 8 and 9, it is observed that the stiffness of beam 1 has a more noticeable drop after initial crack as compared with beam 2. This is due to the presence of stirrups which induce confining action on the concrete in beam 2. The comparison between the observed crack pattern and the computed crack pattern are shown in Fig. 10. It is observed that the prediction of the crack pattern is in reasonable agreement with the measured result.

6. Conclusion

Reinforcement confinement coefficient and an effective method for modelling reinforcement arbitrarily oriented in concrete are proposed in this paper. Two numerical examples showed that the proposed model is reasonable. From laboratory and numerical tests, reinforcement confinement is observed to be important and should be properly considered. The coefficient proposed by the author can be used easily in finite element analysis and offers an attractive way in modelling reinforcement confinement action.

References

Bangash, M. Y. H. (1989), Concrete and concrete structures, *Elsevier Applied Science.*

Bicanic N. (1978), "Nonlinear finite element transient response of concrete structures", Ph.D. Thesis, University of Walse, Swansea.

Bicanic. N. and Zienkiewicz, O. C. (1973), Constitutive model for concrete under dynamic loading, *Earthquake Engng. and Struct.* Dyn., **11**, 689-710.

B. S. 8110 (1985), *Structural use of concrete*, British Standards Institution.

Cheng, Y. M. and Fan, Y. (1994), "Laboratory and numerical test on concrete plank composite with reinforcement truss", *Journal of Structural Engineering*, **20**, 207-216.

Elwi, A. E. and Hrudey, T. M. (1989), "Finite element Modeling for curved embedded reinforcement", *ASCE*, **115**(4), April.

Giuriani, E. *et al*, (1991), "Role of stirrups and residual tensile strength of cracked concrete on bond", *ASCE*, **117**(1), January.

Hinton, E. (1988), Dynamaic analysis of plate and shell, Pineridge Press, Swansea.

Kupfer, H., Hilsdorf, K. H. and Rush, H. (1969) "Behaviour of concrete under biaxial stresses", *Proc. ACI*, **66**, 656-666.

Kupfer *et al*, "Behavior of concrete under biaxial stress", (1969) *ACI. Journal*, **66**(8), Disc. Feb. 1970.

Miyamoto, A. *et al*, (1991), "Nonlinear dynamic analysis of reinforced concrete Slabs under impulsive loads", *ACI*, **88**(4), July-August.

Miyamoto A. *et al*, (1991), "Analysis of Failure modes for reinforced concrete Slabs under impulsive loads", *ACI*, **88**(5), Setember-October.

Perzyna J. (1966), "Fundamental problem in viscoplasticity", *Adv. Appl. Mech.*, 243-377.

Phillips, D. V. and Zienkiewicz, O. C. (1976), "Finite element non-linear analysis of concrete structuress", *Proc. Instn Civ. Engrs.*, Part 2, 59-88.

Yamaguchi, (1991), "An efficient approach to finite element analysis of reinforced concrete", *Proceeding of the Asian Conference on Computational Mechanics*, Hong Kong, Dec., 203-208, 1991.

Zienkiewicz, O. C. and Tylor, R. L. (1991), The finite element method, fourth edition, **2**, McGrw-Hill.